MICTOSTRUCTURAL ANALYSIS OF LASER CLADDING OF STELLITE 6 ON DUCTILE IRON

Ebrahim Harati[1], Farshid Malek Ghaini[2] and Mohammad Javad Torkamany[2]

[1]Department of Engineering Science, University West, SE-461 86 Trollhättan, Sweden. [2]Department of Materials Engineering, Faculty of Engineering, Tarbiat Modares University, Tehran 14115-143, Iran

Ebrahim.harati@hv.se

Abstract: Stellite 6 alloy in the form of powder was deposited on a ductile cast iron substrate using a low power pulsed Nd:YAG laser. The effects of process parameters on the resulting microstructure and hardness were studied with emphasis on the single and multi-track deposits. The results revealed that the cladded layers consist of carbides dispersed in a Co-based solid solution matrix with a dendritic structure. Multi-track cladded layers have coarser dendrites compared to those of single-track cladded layer due to a longer exposure time at high temperature and slower cooling rates as more layers were deposited.

Keywords: Laser Cladding, Stellite 6, Microstructure, Ductile cast iron.

1. INTRODUCTION

Ductile iron (DI) is a ferrous alloy widely used in the manufacturing of machine tool beds, cams, pistons, cylinders, etc., because of low cost, good fluidity and castability, excellent machinability, good mechanical strength and good wear resistance. However, under severe service conditions the performance and reliability of DI can be limited (Arabi Jeshvaghani et al., 2011a). Compared with conventional surface cladding techniques such as Tungsten Inert Gas (TIG) or Plasma Transferred Arc (PTA), the main advantages of laser cladding (Lim, et al., 2008; Toyserkani, et al., 2004; Steen, 1991; Kannatey-Asibu, 2009) are: localized treatment, low heat input, which results in low dilution and low distortion, fine microstructure in the cladded layer, resulting from high cooling rate and high degree of automation which results in high reproducibility. However, because considerable free carbon in the form of graphite flakes presents in cast iron, laser cladding on cast iron cannot be performed easily due to high laser beam absorption of graphite that could create non-homogeneous thermal fields (Ocelík, et al., 2007).

Cobalt based alloys including the Stellite families are widely used for hardfacing. Stellites have high flow stresses and exhibit good resistance to oxidation, erosion, abrasion, and galling at temperatures up to about 90% of their melting temperature. They are primarily used to coat components in the chemical and power generation industries, and are available in powder, rod, electrode, chip, foil, mat and wire forms. Stellite 6 is the most popular alloy in the Stellite families. In this alloy, chromium forms carbides, which strengthen the cobalt matrix. Other elements are added to improve various properties – tungsten and molybdenum have large atomic radii, which distort the lattice providing strength. They also form hard carbides readily (Arabi Jeshvaghani, et al., 2011b; Ion, 2005; Gholipour, et al., 2011; Crook, 1994). A number of practices have been developed by cladding Stellite 6 onto steel substrates. Variations have been developed, mainly to increase the efficiency of alloy usage and to improve the crack resistance. In this regard, Lin and Chen (2006), carried out laser cladding of Stellite 6 alloy on mild carbon steel and found that laser-clad Stellite 6 layer exhibited refined dendritic microstructure and the interdendritic eutectics consisted of either small carbides or intermetallic compounds randomly distributed in a cobalt-rich solid solution. Also, Ocelík, et al. (2007), performed thick Stellite 6 coating on cast iron by a high power continuous Nd:YAG laser. Their findings showed that a wide processing window exists for side-cladding

of Stellite 6 on cast iron substrate and crack-free and macro-pore-free coatings with a thickness up to 3 mm were achieved by subsequent deposition of partially over-lapping laser tracks and by multiple layer cladding.
The current work aims at utilizing pulsed laser cladding method and Stellite 6 alloy powder to deposit single and multi-track coatings on ductile iron and to examine the microstructural characteristics of the coatings.

2. MATERIALS AND METHODS

Stellite 6 powder with mean particle size of 50 µm was used as the cladding material. The substrate (4 mm in thickness) was ductile cast iron. The chemical compositions of the clad powder alloy achieved by using X-ray fluorescence (XRF), the deposited stellite 6 layer obtained by OES and the substrate are listed in Table 1.

Table 1. Chemical composition of the powder alloy, deposited layer and substrate (wt.%).

	Co	Fe	Cr	W	C	Si	Ni	Mn	P
powder alloy	Bal.	2	27	5	1.1	1.6	2.1	0.6	-
deposited layer	Bal.	3.6	26	4.2	1.7	1.2	2	0.8	-
substrate	-	Bal.	-	-	3.7	2.5	-	0.25	<0.05

The cladding operations were performed using IQL-10 machine, a pulse Nd:YAG laser with a maximum mean laser power of 400 W. The focusing optical system is composed of three lenses with 75-mm focal length. A 5000-W Lp Ophir power meter and LA300W-LP Joule meter were used to measure the average power and pulse energy. A gravity based powder feeder was used to feed the powder with a feeding rate of 12 g/min to the interaction region between the laser beam and substrate through a side injecting nozzle. Argon shielding gas was fed along the powder stream. It was also used to protect the optical lenses and prevent the formation of oxides and clad contaminations due to the contact with surrounding. The substrate was moved under the stationary beam by a numerically controlled XYZ table. A view of the experimental setup is presented in Figure 1.

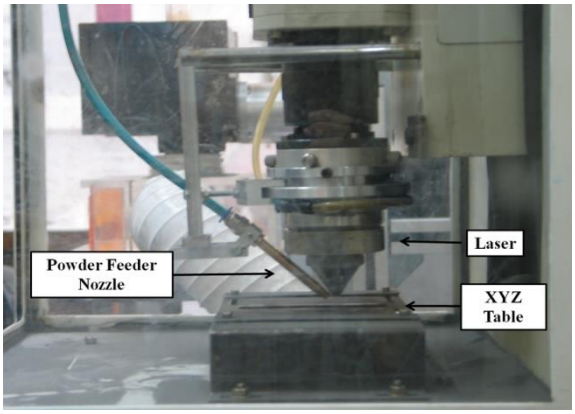

Fig.1. A photographic view of the experimental setup used in the investigation.

Single and multi-track, laser cladded specimens were produced. In each layer, laser power was turned off at the end of each pass and substrate rapidly returned to the new starting position. Consecutive tracks were deposited adjacent to each other starting always on the same side of the specimen. The multi-track was achieved by moving the laser beam at an increment of 1-1.5 mm between each track. Table 2 lists the laser cladding parameters utilized in this investigation.

Table 2. Laser cladding parameters utilized in the investigation.

Laser power	200-220 W
Substrate velocity	1 mm/s
Shield gas flow rate	40-50 L/min
Carrier gas flow rate	15-20 L/min
Laser pulse width	6 ms

The cladded samples were examined by means of optical, chemical, and metallographic methods. After cutting, polishing and etching of the samples the microstructure was investigated by means of optical and scanning electron microscopes as well as X-ray diffraction technique. For chemical analysis energy dispersive spectroscopy (EDS) and Optical Emission Spectroscopy (OES) were applied. Measurements of the Vickers microhardness were made using a load of 300 g in the sample cross-sections vertical to the clad-track directions at different distances from the coating-substrate interface.

3. RESULTS AND DISCUSSION

The cross sections of the cladded samples are shown in Figs. 2(a) and (b).

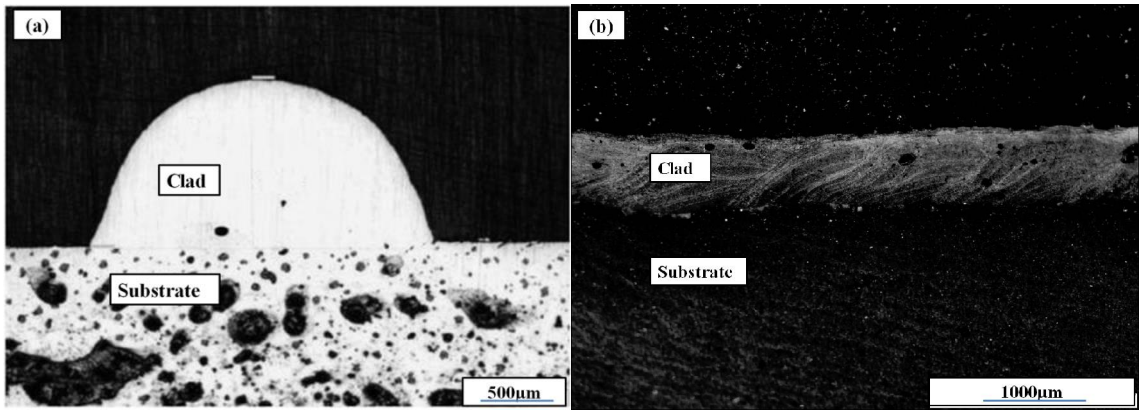

Fig.2. cross sections of the cladded samples: (a) single-track cladded layer, (b) multi-track cladded layer.

Figs. 3(a) and (b) show the microstructure near the interface with the base metal while Figs. 3(c) and (d) show it in the center of the cladded layers for single-track and multi-track specimens, respectively. The as-deposited structures of laser-clad layers comprise of basically a hypoeutectic structure, containing primary dendrites and interdendritic eutectics as reported by Lin and Chen (2006).

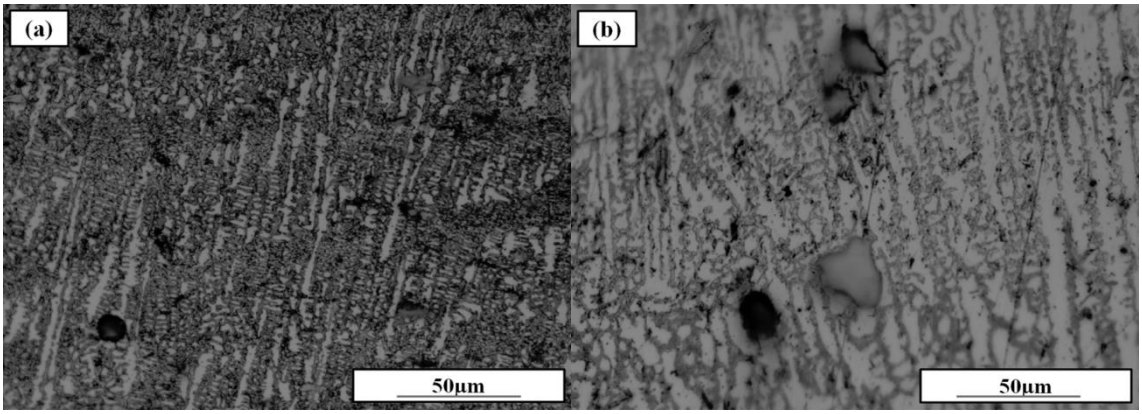

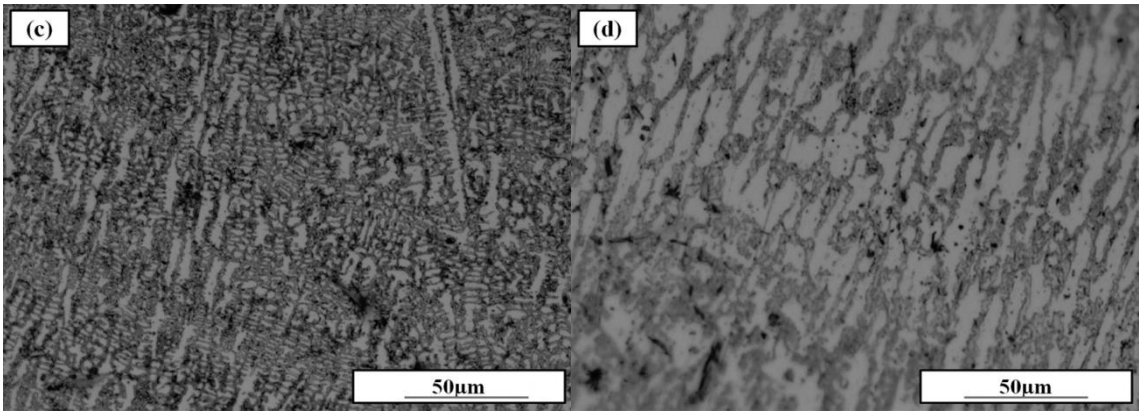

Fig.3. Optical micrograph of cladded layers. (a) Single-track cladded layer near the interface with the base metal, (b) Multi-track cladded layer near the interface with the base metal (c) Single-track cladded layer at the center of the cladded layers, (d) Multi-track cladded layer at the center of the cladded layers.

In comparison with single-track cladding, multi-track cladding involves the overlap of one track by the subsequent track. Multi-track cladded layers had coarser dendrites compared to those of single-track cladded layer attributed to the longer exposure times at elevated temperatures and slower cooling rates as more layers were deposited (Ana Sofia, et al., 2002).

From fusion line toward the centerline, the solidification rate (R) increases and thermal gradient (G) decreases, so that, the (G/R) ratio is higher at the fusion line that results in cellular dendrites near the interface and by approaching coating surface, this ratio gradually becomes lower that causes an epitaxial dendritic structure (Xu, et al., 2006; Jeng, et al., 1991; Kathuria, 2000). In Figs. 4(a) and (b), three distinguished regions of A, B and C, can be seen that belong to the overlapped area of successive laser tracks, the area between two laser pulses in an individual track and the interface between two laser pulses, respectively.

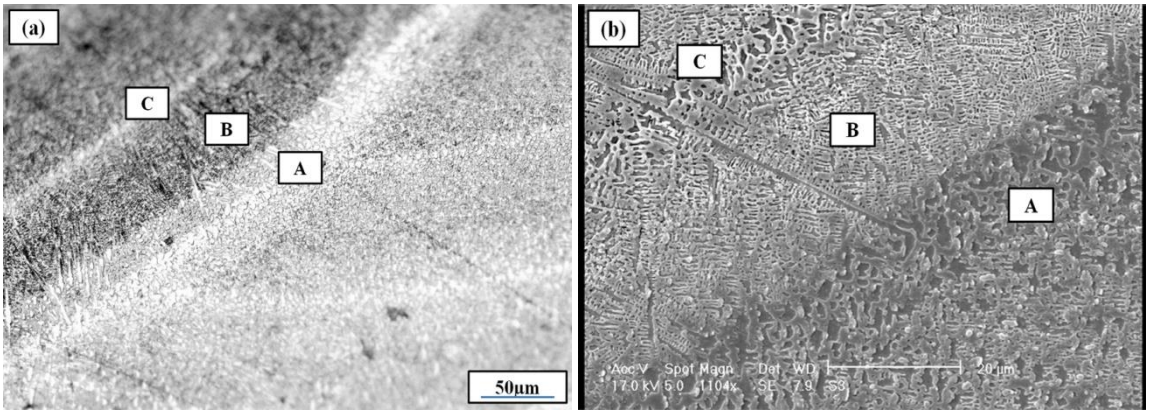

Fig.4. Microstructure in a multi-track cladded layer: A: Overlapped area of successive laser tracks, B: Area between two laser pulses and C: Interface between two laser pulses a) Optical micrograph b) SEM photograph.

In region A, a coarsened structure is observed. This can be related to the remelting of the previous track by the subsequent track. Also, a slightly coarse structure in the pulse bands (region C) is caused by the remelting of previous pulse by the following pulse but the pulse band is much thinner than the track band which can be due to the faster cooling rate in a pulse band than that in a track band. These results are in good agreement with works done by Sun, et al. (2005). Also, by considering Fig.4, it can be concluded that the dendrite arm spacing decreases from the region A to the region C because the dendrite arm spacing decreases with increasing cooling rate (Kou, 2003).

The X-ray diffraction pattern of multi-track cladded specimen shown in Fig. 5 confirms the presence of Co-rich γ phase and carbides such as M7C3 and M23C6 in the cladded layer.

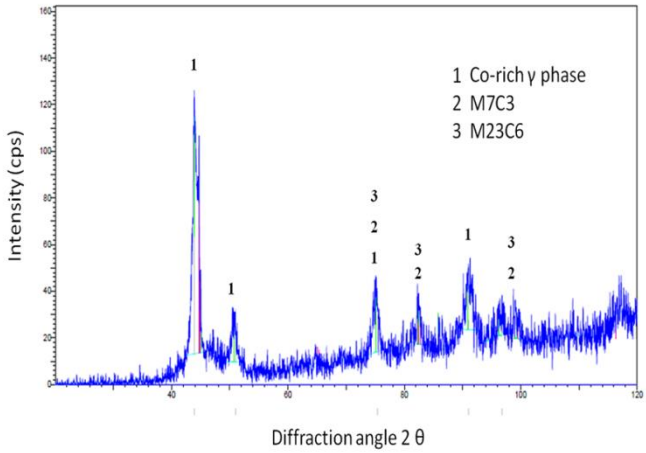

Fig.5. X-ray diffraction analysis of multi-track cladded layer.

Changes in the chemical composition due to laser cladding process were investigated on the basis of optical emission spectroscopy results regarding the major chemical constituents of both substrate and coating. The composition representative of the bulk of the laser-clad obtained from experiment and that corresponding to the original Stellite powder achieved using X-ray fluorescence (XRF) (shown in Table 1), confirmed that during deposition and remelting no significant changes were induced in the chemical composition. Effects of de-alloying or oxidation were not evident.

The EDS quantitative spot analysis of dendritic and interdendritic regions of the single and multi track cladded layers are listed in table 3.

Table 3. The EDS quantitative spot analysis of dendrite and interdendritic regions of the single and multi track cladded layers.

		Elements (wt%)					
		Co	Cr	W	Fe	Ni	Si
Single-track	Dendritic region	Bal.	21.66	2.11	13.64	1.53	1.36
	Interdendritic region	Bal.	32.23	3.09	14.17	0.95	1.76
Multi-track	Dendritic region	Bal.	25.39	3.13	18.13	2.26	1.48
	Interdendritic region	Bal.	33.48	4.44	18.29	1.37	1.58

As can be seen in the table the matrix is relatively richer in Co and the interdendritic region is richer in Cr, W and Si elements for both specimens. Exposure of cobalt base alloys to high temperatures promotes the bulk diffusion of Cr, W and Si elements from dendritic to interdendritic regions, contributing to the increase of very hard carbides such as Cr23C6 and Cr7C3 in these regions. Also, the higher Cr, W and Si elements in the interdendritic regions in multi-track clad is the result of lower cooling rate (i.e. the slower growth of dendrites) in the multi-track clad so that the higher diffusion at the interface between liquid and solid is achieved during solidification.

Therefore one can expect a greater contribution of the interdendritic regions which are richer in these elements to the measured hardness compared with the dendritic regions (Ana sofia, et al., 2002). Also, more contents of Fe and Cr can be seen in interdendritic region for multi-track cladded layer in comparison to those of single-track cladded layer attributed to the longer exposures times at elevated temperature of the multi-track processing. EDS results of dendritic and interdendritic zones for regions A and C illustrated in Fig. 4 are shown in Table 4.

Table 4. The EDS quantitative spot analysis of dendrite and interdendritic regions of the multi-track cladded layer for region A and C illustrated in Fig. 4.

		Elements (wt%)					
		Co	Cr	W	Fe	Ni	Si
Region A	Dendritic region	Bal.	26.87	2.20	20.21	1.43	1.34
	Interdendritic region	Bal.	30.38	2.33	21.20	1.69	1.40
Region C	Dendritic region	Bal.	24.70	2.1	19.29	1.39	0.91
	Interdendritic region	Bal.	27.38	3.70	20.30	2.11	1.67

These results also indicate the presence of slightly more Fe and Cr contents in interdendritic zone in region A compared to those of region C due to the higher exposure times at elevated temperature and lower cooling rate in a track band to that in a pulse band. The microhardness profiles of the cladded layers are presented in Fig. 6.

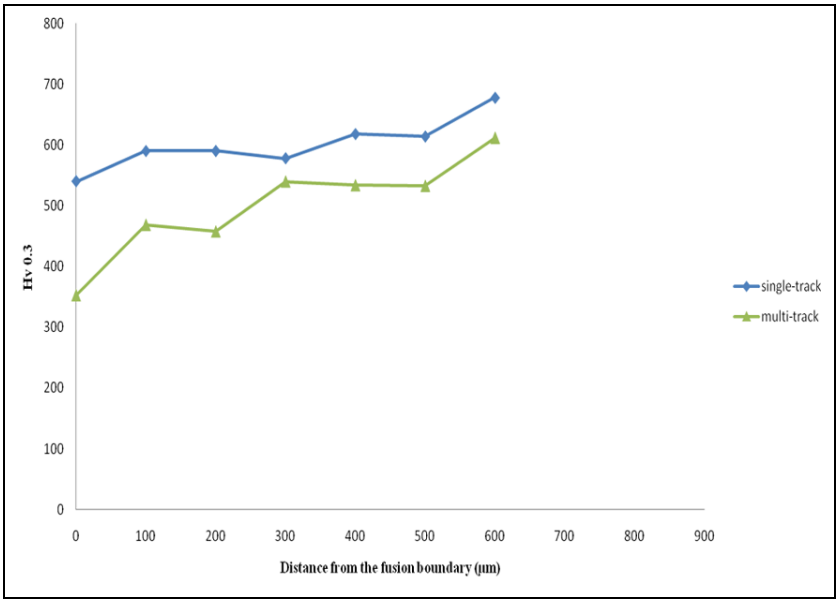

Fig.6. Microhardness profiles for single and multi track cladded layers.

The average Vickers hardness values in single and multi track cladded layers are about 600 and 565 HV, respectively. It can be seen that the cladded layers have higher average hardness in comparison to that of substrate (280 HV). This agrees with the literature and supports the general conclusion that for laser-clads the microhardness values are higher than those of conventional arc welding clads.The high hardness of claddings is derived generally from the high hardness of carbides or intermetallic compounds in the cobalt-rich solid solution (Lin and Chen, 2006). It can also be seen that hardness increases from interface to the surface for both specimens. This is due to the finer size of the grains at the surface in comparison to that at the interface and also the diffusion of Fe adjacent to the interface. Results of EDS line-scan analysis for trend in concentration changes of basic elements across the substrate-clad for multi-track cladded layer confirms the diluted region by Fe in cladded layer (Fig 7).

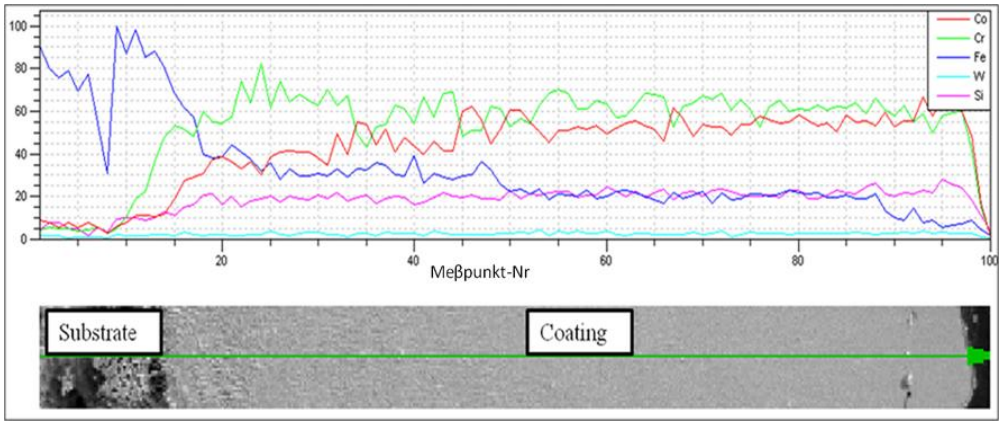

Fig.7. EDS line-scan analysis for trend in concentration changes of basic elements across the substrate-clad for multi-track cladded layer.

Also by considering the microhardness profile, it is clear that the hardness values of single-track cladded layer are higher than those of multi-track cladded layer which can be attributed to the more refined microstructure of single-track cladded layer and also due to the existence of more Fe in multi-track cladded layer. In the case of multi-track cladding, results show soft regions adjacent to harder regions. This dispersion of the measurements as can be seen in Fig 6 is due to the effect of overlapping.

3. CONCLUDING REMARKS

[1] Stellite 6 alloy in the form of powder can be applied on ductile cast iron using a 400W Nd:YAG pulsed laser coupled with a gravity based powder feeder with a feed rate of 12g/minute.

[2] The laser-clad layers comprise of basically a hypoeutectic structure, containing primary Co-rich dendrites and interdendritic eutectics including carbides such as M7C3 and M23C6.

[3] Multi-track cladded layers have coarser dendrites compared to those of single-track cladded layer due to a longer exposure time at high temperature and slower cooling rates as more layers were deposited. Multi-track structures show alternate regions of fine and coarse dendrites, the latter being due to overlapping of the previous tracks by the following tracks.

[4] The high hardness of claddings is derived generally from the high hardness of carbides as well as the refined microstructure of the cladded layers.

[5] Interdendritic and dendritic regions present different chemical compositions, the former being richer in Cr, W and Si and the latter richer in Co and Ni due to the bulk diffusion of Cr, W and Si elements from dendritic to interdendritic regions at high temperatures.

REFERENCES

Ana Sofia C.M. D'Oliveira, P. Se´rgio C.P. da Silva, Rui M.C. Vilar (2002). Microstructural features of consecutive layers of Stellite 6 deposited by laser cladding. *J. Surf.Coat.Technol*. **153**, 203-209.

Arabi Jeshvaghani, R., Harati, E., Shamanian, M. (2011a). Effects of surface alloying on microstructure and wear behavior of ductile iron surface-modified with a nickel-based alloy using shielded metal arc welding. *J. Mater. Design*, **32**, 1531-1536.

Arabi Jeshvaghani, R., Shamanian, M., Jaberzadeh, M. (2011b). Enhancement of wear resistance of ductile iron surface alloyed by stellite 6. *J. Mater. Design*, **32**, 2028-2033.

Crook, P. (1994). *Cobalt and cobalt alloys, ASM Metals. Handbook*, **2** , 10th ed. 658–662. Haynes International, Inc.USA.

Gholipour, A., Shamanian, M., Ashrafizadeh, F. (2011).Microstructure and wear behavior of satellite 6 cladding on17-4 PH stainless steel. *J. Alloy Compd*. **509**, 4905-4909.

Ion, J. C. (2005). Laser processing of engineering materials. Elsevier, Oxford.
Jeng, M. C., Yan, L. Y., Doong, J. L. (1991). Wear behaviour of cobalt-based alloys in laser surface cladding. *J. Surf.Coat.Technol*. **48**, 225-231.
Kannatey-Asibu Jr, E. (2009). Principles of laser materials processing, John Wiley & Sons, New Jersey.
Kathuria, Y.P. (2000). Some aspects of laser surface cladding in the turbine industry, *Surf.Coat.Technol*. **132**, 262-269.
Kou, S. (2003). *Welding Metallurgy*, John Wiley and Sons, New Jersy.
Lim, J. S., Ng, K. L.,The, K. M. (2008). Development of laser cladding and its application to mould repair. *SIMTech*. **9**, 142-147.
Lin, W.C., Chen, C. (2006). Characteristics of thin surface layers of cobalt-based alloys deposited by laser cladding. *J. Surf.Coat.Technol*. **200** , 4557-4563.
Ocelík, V., de Oliveira, U., de Boer, M., de Hosson, J.Th.M. (2007). Thick Co-based coating on cast iron by side laser cladding: Analysis of processing conditions and coating properties. *J. Surf.Coat.Technol*. **201**, 5875-5883.
Sun, S., Durandet, Y., Brandt, M., (2005). Parametric investigation of pulsed Nd: YAG laser cladding of stellite 6 on stainless steel. *J. Surf.Coat.* **194**, 225-231.
Steen, W.M., (1991). *Laser Materials Processing*, Springer, London.
Toyserkani, E., Khajepour, A., Corbin, S. (2004). *Laser Cladding*, CRC Press, Canada.
Xu, G., Kutsuna, M., Liu, Z., Yamada, K., (2006). Comparison between diode laser and TIG cladding of Co-based alloys on the SUS403 stainless steel. *J. Surf.Coat.Technol*. **201**, 1138-1144.